POLITECNICO DI TORINO
Repository ISTITUZIONALE

Novel antibacterial ocular prostheses: proof of concept and physico-chemical characterization

Original
Novel antibacterial ocular prostheses: proof of concept and physico-chemical characterization / Baino, F., Ferraris, S., Miola, M., Perero, S., Verne', E., Coggiola, A., Dolcino, D., Ferraris, M.. - In: MATERIALS SCIENCE AND ENGINEERING. C, BIOMIMETIC MATERIALS, SENSORS AND SYSTEMS. - ISSN 0928-4931. - ELETTRONICO. - 60:(2016), pp. 467-474. [10.1016/j.msec.2015.11.075]

Availability:
This version is available at: 11583/2628024 since: 2016-03-01T15:27:46Z

Publisher:
Elsevier

Published
DOI:10.1016/j.msec.2015.11.075

Terms of use:

This article is made available under terms and conditions as specified in the corresponding bibliographic description in the repository

Publisher copyright

(Article begins on next page)

08 October 2026

Novel antibacterial ocular prostheses: proof of concept and physico-chemical characterization

Francesco Baino[a,*], Sara Ferraris[a], Marta Miola[a], Sergio Perero[a], Enrica Verné[a], Andrea Coggiola[b], Daniela Dolcino[b], Monica Ferraris[a]

[a] *Institute of Materials Physics and Engineering, Applied Science and Technology Department, Politecnico di Torino, Corso Duca degli Abruzzi 24, Torino, Italy*

[b] *Ophthalmology Ward, St. Antonio and Biagio and Cesare Arrigo National Hospital, Via Venezia 16, Alessandria, Italy*

* Corresponding author: Francesco Baino

Tel.: + 39 011 090 4668

Fax: +39 011 090 4624

E-mail: francesco.baino@polito.it

Abstract

Discouraging bacterial colonization of ocular biomaterials and implants is a significant challenge in ophthalmology as infections often lead to the need for secondary surgery, with associated risks and additional stress to patients. In this work we demonstrate for the first time the feasibility of an innovative antibacterial ocular prosthesis produced by depositing a silver nanocluster/silica composite layer on the poly(methyl methacrylate) implant surface via radio-frequency sputtering. Tape test performed according to relevant ASTM standard provided a preliminary evidence of the mechanical stability and good adhesion of the coating to the substrate (absence of macroscopic damage after tape removal). Coating integrity was maintained after prolonged soaking in aqueous medium (1 month). The antibacterial effect of the coating, associated to silver ion release upon

contact with aqueous fluid, was confirmed by the *in vitro* formation of a 5-mm inhibition halo test against *Staphylococcus aureus* that is one of the most common bacteria involved in ocular infections. The approach proposed in the present study for facing implant-related ocular infections can have a significant impact in the field of ophthalmic biomaterials, suggesting a valuable alternative to the administration of antibiotics that may become ineffective due to bacterial resistance.

Keywords: Ophthalmic biomaterial; Coating; Silver; Sputtering; Antibacterial.

1. Introduction

Bacterial issues in ophthalmic applications, with particular reference to postoperative infection of ocular implants, cause significant problems that can require additional, stressful and expensive treatments for the patients [1-6]. In this regard, bacterial infections have dramatic consequences for those patients who underwent enucleation procedures, which involve the removal of the ocular globe due to tumours, oculo-orbital trauma or otherwise untreatable diseases followed by implantation of an artificial eye [7]. In these cases, an orbital implant is inserted in the anophthalmic socket with the aim of filling the orbital volume, allowing normal circulation of tears and supporting the eyelids (Fig. 1a). An aesthetic ocular prosthesis is usually worn by the patient to mimic the features of the normal contralateral eye (Fig. 1b and c).

The most commonly-used orbital implants are designed as porous spheres made of hydroxyapatite, polyethylene or alumina that, once implanted in the patient's ocular socket, are invaded by fibrovascular tissue [8,9]. Poly(methyl methacrylate) (PMMA) is used to produce both serial and custom-made ocular prostheses that are placed between the closed conjunctival surface covering the orbital implant and the eyelid [10]. Usually, the acrylic resin is cast into a properly-designed mould reproducing the exterior features of the patient's eye and the scleral curvature; then, after

polymerization, the final PMMA ocular prosthesis is carefully hand-painted to achieve the best aesthetic effect, i.e. the perfect similarity with the healthy contralateral eye (Fig. 1b).

Over the years, some strategies have been experimented to limit the risk of bacterial colonization at the time of surgery; for instance, it is a common practice to impregnate porous hydroxyapatite orbital implants in antibiotics prior to implantation in the orbital socket [11]. This approach is certainly useful intraoperatively, but a key challenge of modern ophthalmology is to develop smart biomaterials able to exert a long-term antibacterial effect in order to prevent late infections. Moreover, the widespread and increasing use of antibiotics led to the development of antibiotic-resistant bacterial strains, which have been recently indicated as a "global threat" [12]; therefore, there is the need for investigating alternative strategies to treat bacterial infections.

In the literature, there is a relative paucity of publications reporting the development of "smart" ocular devices with antiseptic properties. In a recent patent, Jun et al. [13] disclosed an antibacterial ocular prosthesis produced by incorporating small amounts of silver, gold or platinum nanoparticles in acrylic resin or silicone used to fabricate the prosthesis. Following a similar approach, Yang et al. [14] produced a PMMA-based ocular prosthesis by dispersing silver nanoparticles in acrylic resin (concentration between 300 and 700 ppm) and tested its antibacterial properties *in vitro* against *Streptococcus pneumoniae*, *Staphylococcus aureus*, *Pseudomonas aeruginosa* and *Escherichia coli*. The antimicrobial activity of this Ag-containing artificial eye was significantly stronger than that of as-such polymeric controls. Both approaches, however, pose a serious problems associated to the possible release of nano-sized silver, which could be a crucial issue for the real implant applicability in the clinical practice since many studies have demonstrated the cell/tissue toxicity of metal nanoparticles *in vitro* and *in vivo* [15,16].

Exploiting metal ion release from biomaterial surfaces for antibacterial purposes has been shown to be a valuable and promising strategy, not only in the field of ophthalmology [17]. As to the specific application considered in the present work, it cannot be ignored that the ocular environment is a particularly complex one and several parameters should be taken into account when designing

suitable implants and devices; for instance, the interaction of Ag^+ ions with the tears, the fate of the ions released and the possible ion-induced conjunctival tissue necrosis are all aspects deserving careful consideration in future research. As such a topic is very new, the relevant available literature is quite scarce; Hau and Tuft [18] recently described a case of corneal argyrosis associated with silver nitrate-coated cosmetic soft contact lenses that a 67-year-old woman wore for 17 years for the management of intractable diplopia: this is a typical example of an apparently unexpected side effect detectable only after many years of follow-up.

A promising strategy that has been recently proposed in a patent by Baino et al. [19] involves the deposition of an antibacterial silver nanocluster/silica composite coating on the surface of ocular prostheses by radio-frequency (RF) co-sputtering of silver and silica used as target materials. This strategy is expected to overcome the drawbacks of the antibacterial device proposed by Yang et al. [14], including the toxicity of the released nanosilver and the high cost of the metal nanoparticles to be incorporated in the bulk of the prosthesis. Our approach is founded on the use of RF sputtering, that is recognized as a versatile technique adopted to obtain coatings with different features and intended for a wide range of applications [20,21]; among them, the ability to deposit antibacterial layers on various surfaces for healthcare, clinical or, in general, everyday use has received increasing attention in the last years [22-26]. For the first time, this work reports the feasibility and characterisation of silver nanocluster/silica composite antibacterial coatings deposited on the rear surface of PMMA ocular prostheses to be used in contact with the patient's conjunctiva (Fig. 1a). This approach is novel and, to the best of the authors' knowledge, has never been applied in the field of ocular biomaterials.

2. Materials and methods

2.1. Preparation of the samples

Silver nanocluster/silica composite coatings were deposited by RF co-sputtering of silica and silver (targets) onto PMMA substrates. For the purpose of simplicity, the feasibility of these antibacterial coatings was first explored in a simplified, flat geometry; then, the same processing schedule was applied to real PMMA ocular prostheses (Fig. 1b,c). Before being sputtered, all the samples were cleaned with ethanol; the PMMA ocular prostheses (Zabby's Ophthalmic Instruments and Devices, India) were also cut in four quadrants by means of an automatic cutting machine (Accutom 5, Struers) using a diamond blade (330 CA, Struers). The depositions were performed for 15 or 40 minutes (coated samples will be hereafter referred to as C15 and C40, respectively) with a plasma power of 200 W RF on the silica target (purity 99.9%, Franco Corradi Srl) and 1 W DC on the silver target (purity 99.99%, Sigma-Aldrich). In order to better tailor the amount of silver in the coating, the plasma over the silver target was periodically switched OFF and ON with a duty cycle of 6 – 2 seconds (Ag plasma ON for 2 seconds over a 6-second period). Coating depositions were all performed in pure argon atmosphere.

2.2. Characterisation studies

Morphological and compositional investigations of the coatings were carried out by field-emission scanning electron microscopy (FESEM, SUPRA^{TM} 40, Zeiss) equipped with X-ray energy dispersive spectroscopy (EDS); the samples were chromium-coated before the analysis.

The adhesion of the coating to PMMA flat substrate was evaluated by tape test (Fig. 2) according to the ASTM D 3359 standard [27]. The aim of this test is to measure (semi-quantitatively) the strength of a film deposited on a substrate; specifically, it is possible to define the resistance category of the coating by analysing the macro-damages of the film.

Silver release from the coatings was estimated by soaking sputtered quadrants of PMMA ocular prostheses in double-distilled water used as a testing medium. Specifically, four samples (quadrants of prosthesis) per type (C15 and C40) were immersed in double-distilled water contained in

polyethylene flasks (25 ml for each sample, static conditions) at 37 °C up to 1 month. The amount of silver released in the solution was measured at different time points, namely 3 h, 1, 2, 7, 14 and 28 days. At each time point the samples were extracted from the solution and immersed in 25 ml of fresh one. The solution was analyzed in order to determine the silver content by means of a specific spectrophotometer (HI 93737, Hanna Instruments) after the addition of proper reagents (HI93737-03 Kit Silver reagents 150 TEST). The reaction between silver (in the solution) and the reagents causes an orange coloration that can be used to determine the concentration of silver by the spectrophotometer. The method is an adaptation of the 1-(2-pyridylazo)-2-naphthol (PAN) technique [28]. Data were expressed as mean ± SD (calculated on four measurements) of the silver released per unit area of the ocular prosthesis (coated with the silver/silica layer and exposed to the testing solution). Results were analyzed by Student's t-test; statistical significance was set at $p < 0.05$.

EDS analyses were also performed in order to determine the silver and silicon amount in the coating before immersion and after the whole soaking period (1 month).

Assessment of the antibacterial effect of the coatings was performed by the inhibition halo test, according to the protocols of the National Committee for Clinical Laboratory Standards (NCCLS) [29] by using *Staphylococcus aureus* strain (ATCC 29213). *Staphylococcus aureus* was selected as it is one of the most important and common human bacterial pathogens involved in ocular infections [30]. Briefly, a 0.5 McFarland suspension, containing approximately 1.5×10^8 colony forming units (CFU)/ml was prepared and uniformly spread on Mueller Hinton agar plate; the samples were placed in contact with the agar and incubated overnight at 37 °C. After incubation for 24 h, the inhibition halo was observed and measured. Test was performed in triplicate; pure (non-coated) PMMA was used as a control.

3. Results and discussion

A typical PMMA ocular prosthesis used in this work is shown in Fig. 1b and c; Fig. 1d displays the morphology of the polymeric surface to be coated. Quadrants of the PMMA ocular prostheses that underwent coating deposition are shown in Fig. 3; from a qualitative viewpoint, it is possible to observe that a higher deposition time (40 min vs. 15 min) is associated to a darker colour of the sputtered surface due to the higher silver content in the coating.

The surfaces of the coatings were investigated by FESEM and revealed an irregular, cauliflower-like morphology typical of sputtered silica with silver nanoclusters visible as bright "dots" (Fig. 4a). Average size of silver nanoclusters was around 10 nm, as roughly estimated by the high-magnification micrograph reported in Fig. 4b. The EDS analysis (Table 1) revealed Ag/Si atomic ratios of 0.29 and 0.45 for C15 and C40 samples, respectively; these quantitative findings are consistent with the qualitative observations reported in Fig. 3.

The results of the tape test are shown in Fig. 5: the application and subsequent removal of the tape from the surface of the coated PMMA flat sample, after the incision of a grid of parallel cuts on the surface, induced no alteration of the coating both inside and outside the grid compared to the sample before the test. No traces of the coating, which might have been removed partially by the tape, were found on the tape surface after the test. Therefore, according to the ASTM D 3359 standard [27], the sample can be classified as belonging to the 5B class (no damage), which demonstrates a good adhesion of the silver nanocluster/silica composite coating to the PMMA substrate.

As to the soaking test in double-distilled water, Fig. 6 shows a progressive discoloration of the sample surface during the immersion period. After 28 days, the C15 sample surface is almost white, whereas the C40 one still maintains a brownish appearance.

As demonstrated by the surface investigations (FESEM analyses) reported in Fig. 7, after 28 days of immersion in double-distilled water the silver nanocluster/silica composite coatings are still visible on the surface of both samples (C15 and C40) and exhibit a morphology unaltered with respect to that of as-deposited coatings (Fig 4a). EDS analyses (Table 1) showed that at the end of the testing

period (28 days) the Ag/Si atomic ratios decreased to 0.09 and 0.21 for C15 and C40 samples, respectively. These results suggest that the coating discoloration illustrated in Fig. 6 is due to progressive silver depletion from the coating; in fact, the brown colour of the coating is attributed to the presence of silver nanoclusters, whereas the silica matrix is almost colourless.

The antibacterial activity of silver is related to the progressive release of Ag^+ ions into the body fluids; then, the amount of silver released from the coating into the testing medium at different experimental times was assessed by a specific spectrophotometer for Ag^+ ions and the obtained results are reported in Fig. 8. The cumulative release was calculated by summing up the silver content in the solutions assessed at the different time points; the obtained curves are shown in Fig. 9. The C15 samples seemed to have completely released the silver contained in the coating at the end of the testing period (silver was almost totally depleted after 14 days of soaking in double-distilled water), whereas the C40 samples were still releasing silver after 1 month; these results are consistent with the qualitative observations illustrated in Fig. 6 and the EDS analyses performed on the sample surface at the end of the testing period (Table 1).

Best fitting of the experimental data plotted in Fig. 9 can be performed by using a logarithmic interpolating function:

$$c = A \ln t + B \tag{1}$$

wherein c (μg cm^{-2}) is the cumulative amount of silver released per unit area of the ocular prosthesis, t is the soaking time, A and B are the model constants.

The interpolating functions and the coefficients of determination R^2 for the C15 and C40 samples are, respectively, the following:

$$c_{C15} = 55.64 \ln t + 58.46 \qquad (R^2 = 0.9416) \tag{2}$$

$$c_{C40} = 141.09 \ln t - 29.93 \qquad (R^2 = 0.9893) \tag{3}$$

Fitting results exhibit good agreements with experimental data, as demonstrated by the high values of the coefficients R^2, which also reveal the good predictive capability of the presented approach.

For the purpose of discussion, it is instructive to compare the results from the leaching test obtained in the present work with those reported by other authors and concerning the antibacterial effect of silver. Berger et al. [31] reported that the minimum inhibitory concentration (MIC) of Ag^+ ions for various strains of *Staphylococcus aureus* is in the 0.03-0.25 μg ml^{-1} range. Cumulative silver ion releases (mean values) at 24 h were around 0.34 and 0.60 μg ml^{-1} for C15 and C40 samples, respectively; therefore, comparison between these data and the reference ones [31] suggests that the coated ocular prostheses could exhibit an antibacterial effect. This hypothesis is in full accordance with the experimental evidence obtained from the antibacterial test. The antibacterial effect of C15 samples was demonstrated by the inhibition zone test (Fig. 10): Ag^+ ions, deriving from the nanoclusters embedded in the composite coating (shown in Fig. 4b) diffused into the culture agar and were responsible for the formation of a reproducible and significant inhibition halo of about 5.0 ± 0.5 mm around the samples (Fig. 10a). Fig. 10b shows that this halo can be divided in two zones: the bacterial proliferation was totally inhibited near to the sample (1.5 ± 0.5 mm), whereas a limited bacterial growth was observed in the peripheral region of the halo (2 to 5 mm from the sample). As expected, pure PMMA tested as a control was unable to create an inhibition zone.

It is instructive to underline that *Staphylococcus aureus* is a Gram-positive bacterium and it is known that Gram-positive bacteria are less susceptible to antibacterial agents than Gram-negative strains [32,33]. Therefore, being the silver nanocluster/silica composite coating effective against *Staphylococcus aureus*, it is expected to have an even more significant antibacterial effect towards Gram-negative bacterial strains, too.

A preliminary indication about the potential toxicity of the sputtered surfaces investigated in the present work can be provided through a comparison with available data from the literature. The cytotoxicity threshold of silver ions (for L929 fibroblasts) has been estimated to be 0.0035 mmol l^{-1} [34], which is slightly higher than the average value of cumulative release from C15 samples at 24 h (0.003151 mmol l^{-1}). In the case of C40 samples, the threshold value is overcome after 24 h (0.005375 mmol l^{-1}), which suggests the risk of cell toxicity. However, the silver release *in vitro*

cannot be directly related to an *in vivo* behaviour, because of the different boundary conditions involving the turnover of biological fluids (tears) in the ocular environment; furthermore, the different chemical composition between real physiological fluids (tears) and the model fluid used in the present work (double-distilled water) may result in different release kinetics. Therefore, testing in double-distilled water gives only an approximate estimate of what may occur in an *in vivo* scenario.

It cannot be ignored that under physiological conditions, i.e. in the presence of biological fluids containing chloride ions and proteins, a rapid conversion of Ag ions to AgCl and Ag-organo-complexes will occur, which can reduce the biological activity [35,36].

As far as the safety of the coating is concerned, it is worth pointing out that silver nanoclusters are embedded in the silica matrix in a stable way and only silver ions are released but not nanoparticles, as recently observed by Ferraris et al. who investigated the suitability of analogous coatings for different substrates and applications [37].

From the above-reported preliminary results, the silver nanocluster/silica composite coatings produced in this work can be considered potentially suitable for the intended application on ophthalmic implants, as they elicit a good antibacterial effect against *Staphylococcus aureus,* one of the pathogenic strain most involved in the development of biomaterial-associated infection development [38], and exhibit a satisfactory adhesion to the PMMA substrate as well as stability upon prolonged soaking in aqueous media. *In vitro* biocompatibility of silver nanocluster/silica composite coatings has been evaluated on other polymeric substrates in a previous work with promising results [39].

4. Limitations of the present study and future work

This study is limited by the low sample number in all experiments, which is mainly related to the difficult availability and high cost of high-quality ocular prostheses. Therefore, we would like to

emphasise that more detailed antibacterial and biological tests with larger sample number are required to fully elucidate and prove the antiseptic effect and tissue response of the present silver nanoscluster/silica-coated ocular prosthesis.

Evidence of the antibacterial effect of the coating has been provided by the inhibition halo test; additional microbiological tests could be performed in a dedicated study. On the other hand, the ability of analogous coatings to reduce bacterial adhesion was already demonstrated in a previous work [40].

The biocompatibility of PMMA is well-recognized from decades and that of analogous silver/silica coatings has been recently proven *in vitro* in a previous work [39]. To the best of the authors' knowledge, no specific biological test is recommended in the literature or is routinely applied to assess the biocompatibility of ocular prostheses. This is probably due to the paucity of innovation in the field and the common use of highly biocompatible PMMA for such an application. In general, advanced biological *in vitro* tests on ophthalmic biomaterials are relatively scarce in the literature, probably due to the difficult availability of appropriate ocular cell types that often derive from surgical discard (very delicate primary cells). In this regard, human orbital fibroblasts were occasionally used in contact with orbital implant materials [41] and keratocytes were employed to characterize the *in vitro* biocompatibility of artificial corneas [42,43]. As ocular prostheses are intended to be in contact with the patient's conjunctiva, the use of epithelial cells could be suggested for detailed *in vitro* testing in a future work.

We would like to point out that the cytotoxicity also depends on the amount/releasing profile of silver ions. A systematic study focusing on the influence of different silver amount in the coating as well as the silver release profiles on cytotoxicity remains to be done.

Cytotoxicity testing with appropriate cell types is useful to avoid unnecessary, time-consuming and expensive animal experiments. However, according to most scientists, there is no recognized alternative to pre-clinical animal trials in order to progress the development of biomedical implants towards the final stage of clinical trials (human patients). The ideal implantation site for ophthalmic

biomaterials is the eye with its unique physiological and microenvironmental characteristics; however, this requires the expertise and availability of a skilled ophthalmic surgeon to perform operation [44]. In order to simplify the experiments, some authors proposed a rabbit skin subcutaneous model to investigate the *in vivo* biocompatibility of ophthalmic biomaterials for artificial cornea [45]; a similar approach could be also followed in the future to test the antibacterial biomaterials proposed in the present work. Another important issue is the investigation of the systemic/organ toxicity induced by the degradation products (including ions) released by implanted biomaterials. A recent, pilot study by Yun et al. [46] – although dealing with a non-ocular application – could be considered as a starting point for future work.

5. Conclusions

In this work, antibacterial properties were imparted for the first time to a polymeric ocular prosthesis by means of silver nanocluster/silica composite coatings deposited by RF sputtering. The antibacterial activity was related to the ability of the coated samples to release silver ions in solution, as verified by leaching tests. The coated samples were able to produce a significant inhibition halo against *Staphylococcus aureus*. The coatings were mechanically well-adherent to PMMA substrates. The use of metal ions as antibacterial agents instead of antibiotics, which are commonly employed in therapy and for the prevention of implant-related infections, could overcome the problem of bacterial resistance and could also be effective on resistant bacterial strains.

The results reported in this study are promising and encourage further research, which should involve the cross-fertilization among different disciplines. In the next few years, ever increasing cooperation between materials scientists, chemists, biologists, ophthalmic surgeons and researchers working in the medical implant industry would be more than desirable for the selection and

marketing of more suitable and cost-effective biomaterials for managing the anophthalmic socket in order to further improve the patient's quality of life.

Acknowledgements

This work was partially supported by the Regione Piemonte (Italy) (Regional Project "NABLA" – Nanostructured Antibacterial Layers) and by the EC-funded Project NASLA-FP7-SME-2010-1 (Project no. 262209).

References

[1] S.J. You, H.W. Yang, H.C. Lee, S.J. Kim, Five cases of infected hydroxyapatite orbital implant, J. Kor. Ophthalmol. Soc. 43 (2002) 1553–1557.

[2] J.R.You, J.H. Seo, Y.H. Kim, W.C. Choi, Six cases of bacterial infection in porous orbital implants, Jpn. J. Ophthalmol. 47 (2003) 512–518.

[3] S. Karsloglu, D. Serin, I. Simsek, S. Ziylan, Implant infection in porous orbital implants, Ophthal. Plast. Reconstr. Surg. 22 (2006) 461–466.

[4] D.R. Jordan, S. Brownstein, J. Robinson, Infected aluminum oxide orbital implant, Ophthal. Plast. Reconstr. Surg. 22 (2006) 66–67.

[5] D.R. Jordan, S. Brownstein, N. Rawlings, J. Robinson, An infected porous polyethylene orbital implant, Ophthal. Plast. Reconstr. Surg. 23 (2007) 413–415.

[6] J.Y. Chuo, P.J. Dolman, T.L. Ng, F.V. Buffam, V.A. White, Clinical and histopathologic review of 18 explanted porous polyethylene orbital implants, Ophthalmology 116 (2009) 349–354.

[7] D.M. Moshfeghi, A.A. Moshfeghi, P.T. Finger, Enucleation, Surv. Ophthalmol. 44 (2000) 277-301.

[8] R. Chalasani, L. Poole-Warren, R.M. Conway, B. Ben-Nissan, Porous orbital implants in enucleation: a systematic review, Surv. Ophthalmol. 52 (2007) 145–155.

[9] F. Baino, C. Vitale-Brovarone, Bioceramics in ophthalmology, Acta Biomater. 10 (2014) 3372–3397.

[10] F. Baino, S. Perero, S. Ferraris, M. Miola, C. Balagna, E. Verné, C. Vitale-Brovarone, A. Coggiola, D. Dolcino, M. Ferraris, Biomaterials for orbital implants and ocular prostheses: overview and future prospects, Acta Biomater. 10 (2014) 1064–1087.

[11] J. Badilla, P.J. Dolman, Methods of antibiotic instillation in porous orbital implants, Ophthal. Plast. Reconstr. Surg. 24 (2008) 287–289.

[12] P. Stephens, Antibiotic resistance now 'global threat', WHO warns. BBC News Health, April 30, 2014. Webpage: http://www.bbc.com/news/health-27204988.

[13] M.S. Jun, J.H. Jun, S. Jun, Y.M. Jun, Bio-artificial eye and conformer. US Patent No. US2008/0262612A1 (2008).

[14] J.W. Yang, J.W. Choi, S.G. Lee, D.S. Kim, Antibacterial properties of artificial eyes containing nano-sized particle silver, Orbit 30 (2011) 77–81.

[15] K. Kawata, M. Osawa, S. Okabe, In vitro toxicity of silver nanoparticles at noncytotoxic doses to HepG2 human hepatoma cells, Envir. Sci. Technol. 43 (2009) 6046–6051.

[16] A. Haase, J. Tentschert, H. Jungnickel, P. Graf, A. Mantion, F. Draude, J. Plendl, M.E. Goetz, S. Galla, A. Masic, A.F. Thuenemann, A. Taubert, H.F. Arlinghaus, A. Luch, Toxicity of silver nanoparticles in human macrophages: uptake, intracellular distribution and cellular response, J. Phys. Conf. Series 304 (2011) 012030.

[17] A. Hoppe, N. Guldal, A.R. Boccaccini, A review of the biological response to ionic dissolution products from bioactive glasses and glass-ceramics, Biomaterials 32 (2011) 2757–2774.

[18] S.C. Hau, S.J. Tuft, Presumed corneal argyrosis from occlusive soft contact lenses: a case report, Cornea 28 (2009) 703–705.

[19] F. Baino, S. Perero, M. Miola, S. Ferraris, E. Verné, M. Ferraris, Rivestimenti e trattamenti superficiali per impartire proprietà antibatteriche a dispositivi per oftalmoplastica, IT0001412705 (2012).

[20] P.J. Kelly, R.D. Arnell, Magnetron sputtering: a review of recent developments and applications, Vacuum 56 (2000) 159–172.

[21] H. Biederman, RF sputtering of polymers and its potential application, Vacuum 59 (2000) 594–599.

[22] S.B. Sant, K.S. Gill, R.E. Burrell, Nanostructure, dissolution and morphology characteristics of microcidal silver films deposited by magnetron sputtering, Acta Biomater. 3 (2007) 341–350.

[23] H.B. Wang, Q.F. Wei, J.Y. Wang, J.H. Hong, X.Y. Zhao, Sputter deposition of nanostructured antibacterial silver on polypropylene non-wovens, Surf. Eng. 24 (2008) 70–75.

[24] M. Ferraris, S. Perero, M. Miola, S. Ferraris, E. Verné, J. Morgiel, Silver nanocluster-silica composite coatings with antibacterial properties, Mater. Chem. Phys. 120 (2010) 123–6.

[25] M. Ferraris, C. Balagna, S. Perero, M. Miola, S. Ferraris, F. Baino, A. Battiato, C. Manfredotti, E. Vittone, E. Verné, Silver nanocluster/silica composite coatings obtained by sputtering for antibacterial applications, IOP Conf. Series Mater. Sci. Eng. 40 (2012) 012037.

[26] C. Balagna, S. Ferraris, S. Perero, M. Miola, F. Baino, A. Coggiola, D. Dolcino, A. Battiato, C. Manfredotti, E. Vittone, E. Verné, M. Ferraris, Silver nanocluster/silica composite coatings obtained by sputtering for antibacterial applications, in: J. Njuguna (Ed.), Structural Nanocomposites – Perspectives for Future Applications, Springer-Verlag, Berlin, 2013, pp. 225–247.

[27] ASTM D 3359 (2009) Standard Test Methods for Measuring Adhesion by Tape Test.

[28] http://shop.hannainst.com/hi93737-03-silver-reagents-150-tests.html?id=020&ProdCode=HI%252093737-03 (accessed 25th May 2015)

[29] NCCLS M2-A9. Performance Standards for Antimicrobial Disk Susceptibility Tests. Approved Standard. 9th Edition.

[30] C.C. Chuang, C.H. Hsiao, H.Y. Tan, D.H.K. Ma, K.K. Lin, C.J. Chang, Y.C. Huang, Staphylococcus aureus ocular infection: methicillin-resistance, clinical features, and antibiotic susceptibilities, Plos One 8 (2012) e42437

[31] T.J. Berger, J.A. Spadaro, S.E. Chapin, R.O. Becker, Electrically generated silver ions: quantitative effects on bacterial and mammalian cells, Antimicrob. Agents Chemother. 9 (1976) 357–358.

[32] W.K. Jung, H.C. Koo, K.W. Kim, S. Shin, S.H. Kim, Y.H. Park, Antibacterial activity and mechanism of action of the silver ion in Staphylococcus aureus and Escherichia coli, Appl. Environ. Microbiol. 74 (2008) 2171–2178.

[33] Q.L. Feng, J. Wu, G.Q. Chen, F.Z. Cui, T.N. Kim, J.O. Kim, A mechanistic study of the antibacterial effect of silver ions on Escherichia coli and Staphylococcus aureus, J. Biomed. Mater. Res. 52 (2000) 662–668.

[34] F. Heidenau, W. Mittelmeir, R. Detsch, M. Haenle, F. Stenzel, G. Ziegler, H. Gollwitzer, A novel antibacterial titania coating: metal ion toxicity and in vitro surface colonization, J. Mater. Sci. Mater. Med. 16 (2005) 883–888.

[35] A. Gupta, M. Maynes, S. Silver, The effects of halides on plasmid silver resistance in Escherichia coli, Appl. Environ. Microbiol. 64 (1998) 5042-5045.

[36] S. Silver, Bacterial silver resistance: molecular biology and uses and misuses of silver compounds, FEMS Microbiol. Rev. 27 (2003) 341-353.

[37] S. Ferraris, S. Perero, M. Miola, E. Verné, A. Rosiello, V. Ferrazzo, G. Valletta, J. Sanchez, M. Ohrlander, S. Tjörnhammar, M. Fokine, F. Laurell, E. Blomberg, S. Skoglund, I. Odnevall Wallinder, M. Ferraris, Chemical, mechanical and antibacterial properties of silver nanocluster/silica composite coated textiles for safety systems and aerospace applications, Appl. Surf. Sci. 317 (2014) 131–139.

[38] M.E. Falagas, S.K. Kasiakou, Mesh-related infections after hernia repair surgery, Clin. Microb. Inf. 11 (2005) 3–8.

[39] G. Muzio, S. Perero, M. Miola, M. Oraldi, E. Paiuzzi, S. Ferraris, E. Verné, V. Festa, F. Festa, R.A. Canuto, et al., Biocompatibility and antibacterial properties of polypropylene prostheses coated with silver for hernia repair. Hernia (in press).

[40] M. Miola, S. Perero, S. Ferraris, A. Battiato, C. Manfredotti, E. Vittone, D. Del Vento, S. Vada, G. Fucale, M. Ferraris, Silver nanocluster-silica composite antibacterial coatings for materials to be used in mobile telephones, Appl. Surf. Sci. 313 (2014) 107-115.

[41] L.A. Mawn, D.R. Jordan, S. Gilberg, Proliferation of human fibroblasts in vitro after exposure to orbital implants, Can. J. Ophthalmol. 36 (2001) 245–251.

[42] S.R. Sandeman, A.W. Lloyd, B.J. Tigheb, V. Franklin, J. Li, F. Lydon, C.S.C. Liu, D.J. Mann, S.E. James, R. Martin, A model for the preliminary biological screening of potential keratoprosthetic biomaterials, Biomaterials 24 (2003) 4729–4739.

[43] X.W. Tan, A.P.P. Perera, A. Tan, D. Tan, K.A. Khor, R.W. Beuerman, Comparison of candidate materials for a synthetic osteo-odonto-keratoprosthesis device, Invest. Ophthalmol. Vis. Sci. 52 (2011) 21–29.

[44] F. Baino, How can bioactive glasses be useful in ocular surgery?, J. Biomed. Mater. Res. A 103 (2015) 1259–1275.

[45] X.W. Tan, E.W. Beuerman, Z.L. Shi, K.G. Neoh, D. Tan, K.A. Khor, J.S. Mehta, In vivo evaluation of titanium oxide and hydroxyapatite as an artificial cornea skirt, J. Mater. Sci.: Mater. Med. 23 (2012) 1063–1072.

[46] H.S. Yun, J.W. Park, S.H. Kim, Y.J. Kim, J.H. Jang, Effect of the pore structure of bioactive glass balls on biocompatibility in vitro and in vivo, Acta Biomater. 7 (2011) 2651–2660.

Figure captions

Fig. 1. Devices for oculoplasty: (a) scheme of application (1 = orbital implant substituting the ocular globe removed after enucleation, 2 = patient's conjunctiva, 3 = ocular prosthesis, 4 = antibacterial silver nanosclusters/silica composite coating deposited on the prosthesis surface in contact with the conjunctiva; this idea is proposed in this work for the first time); (b) visual appearance of a poly(methyl methacrylate) ocular prosthesis (or "scleral shell") mimicking the aesthetics of normal eye; (c) rear region of the ocular prosthesis intended to be put in contact with the conjunctiva and to be coated (in the present work) with the antibacterial silver nanosclusters/silica composite layer; (d) FESEM micrograph of the rear surface of the prosthesis used in this work (magnification 50000×).

Fig. 2. Scheme of tape test procedure on coated samples.

Fig. 3. Visual appearance of the ocular prostheses after the deposition of silver nanosclusters/silica composite coatings (deposition time: 15 or 40 minutes) on the rear surface of the PMMA prosthesis.

Fig. 4. Morphological analyses on a coating produced with a deposition time of 15 min (samples C15): (a) and (b) FESEM micrographs of the silver nanosclusters/silica composite coating surface at different magnifications (figure (b) is in back-scattering mode and the contrast is emphasized in order to highlight the presence of silver nanoclusters, that are visible as bright spots). Magnifications: (a) 700000×, (b) 900000×.

Fig. 5. Tape test results on a flat silver nanocluster/silica composite coated C15 sample (deposition time: 15 min).

Fig. 6. Silver nanocluster/silica composite coatings on ocular prostheses: visual appearance after different soaking times in double-distilled water (deposition time of the coating: 15 and 40 minutes).

Fig. 7. Analysis of the surface of the silver nanocluster/silica composite coatings after soaking of the ocular prostheses for 28 days in double-distilled water: (a) and (b) C15 sample; (c) and (d) C40 sample. Magnifications: (a) and (c) 50000×, (b) and (d) 500000×.

Fig. 8. Silver ion release from silver nanocluster/silica composite coated ocular prostheses (deposition time of the coatings: 15 and 40 min) after different soaking times in double distilled water ($p < 0.05$ for C15 vs C40 at each time point).

Fig. 9. Cumulative silver release (in double-distilled water) from the silver nanocluster/silica composite coated ocular prostheses. The fitting curves ("theo") are compared to experimental data ("exp").

Fig. 10. Inhibition halo test by using *Staphylococcus aureus* strain to evaluate the antibacterial activity of the silver nanocluster/silica composite coated samples: (a) general view of a C15 sample (deposition time of the coating: 15 min) and (b) magnification of the inhibition halo that can be divided in two regions: 1 = zone of complete bacterial inhibition, 2 = zone wherein limited bacterial growth is allowed.

Tables

Table 1. Compositional assessment (at.%) of the coatings (EDS). Analyses were performed on three regions of the coating and are expressed as mean ± SD.

Sample	Si	Ag
C15 as such	77.5 ± 2.2	22.5 ± 1.5
C40 as such	68.9 ± 2.1	31.1 ± 1.7
C15 after 28 days in double-distilled water	91.7 ± 2.8	8.3 ± 1.5
C40 after 28 days in double-distilled water	82.6 ± 2.7	17.4 ± 1.2

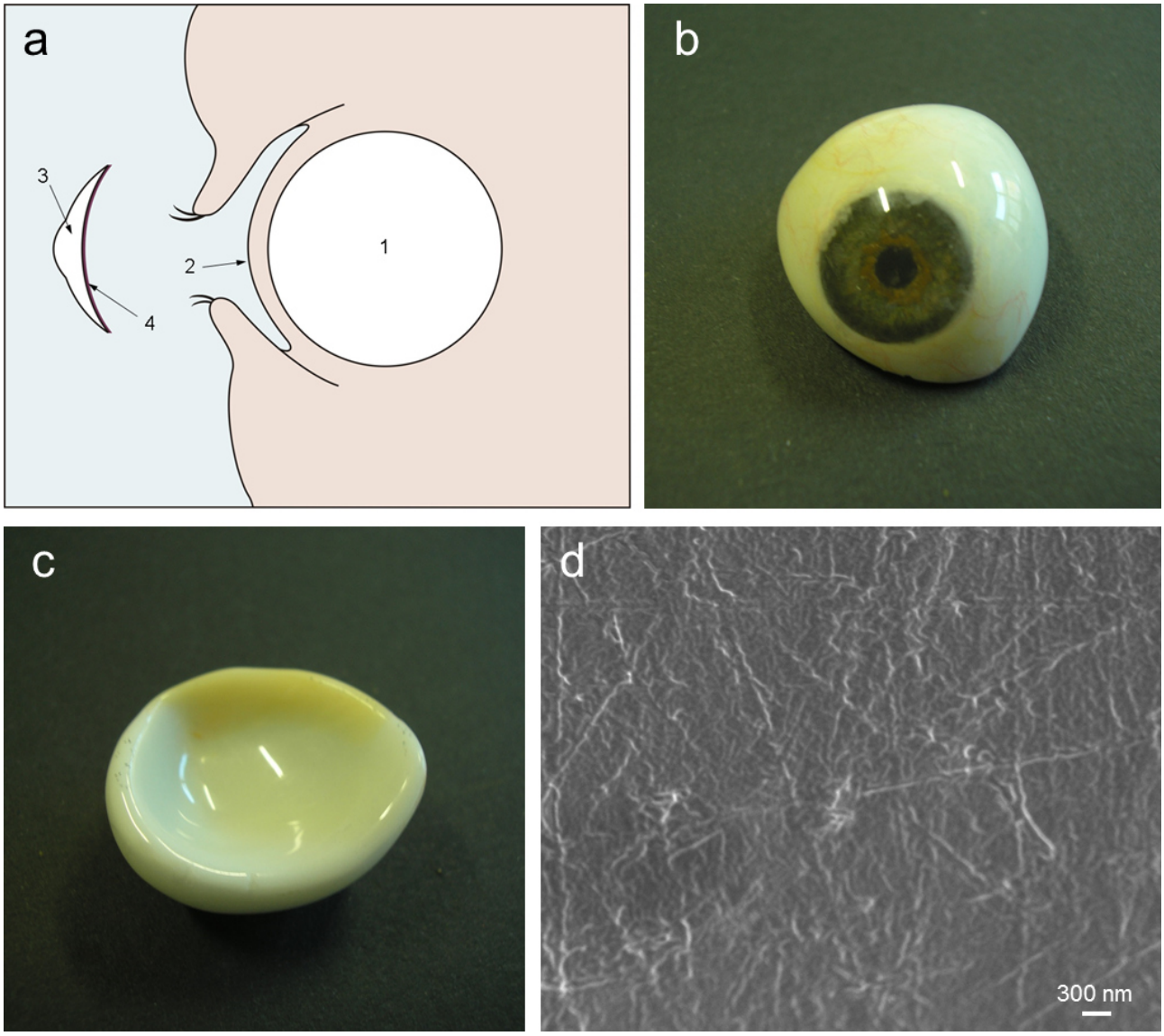

Fig. 1

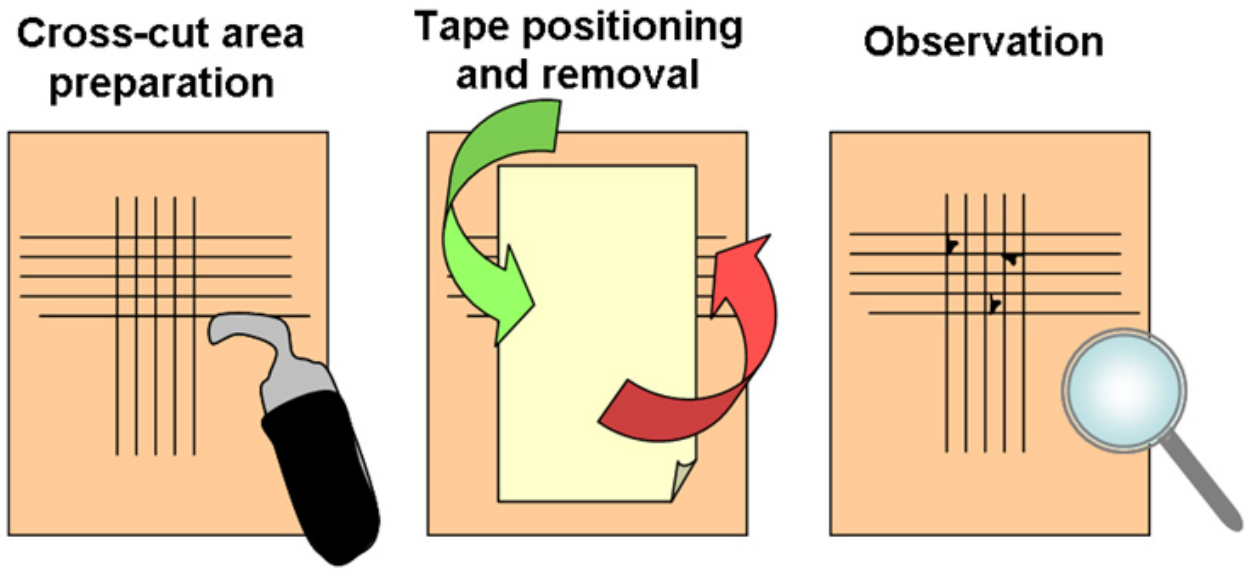
Cross-cut area preparation
Tape positioning and removal
Observation

Fig. 2

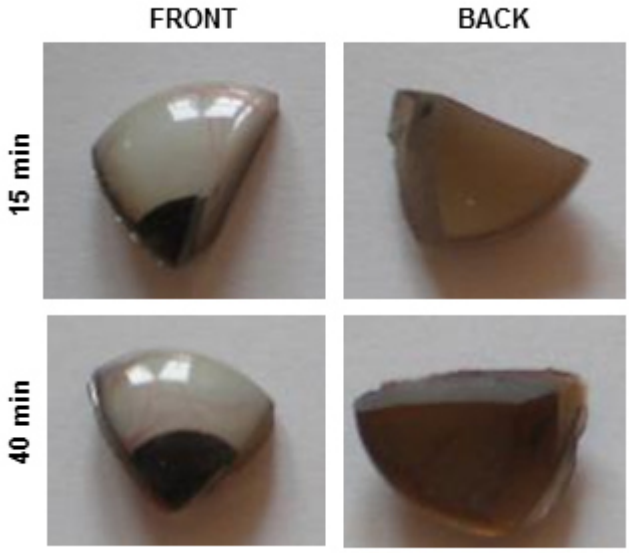
FRONT
BACK
15 min
40 min

Fig. 3

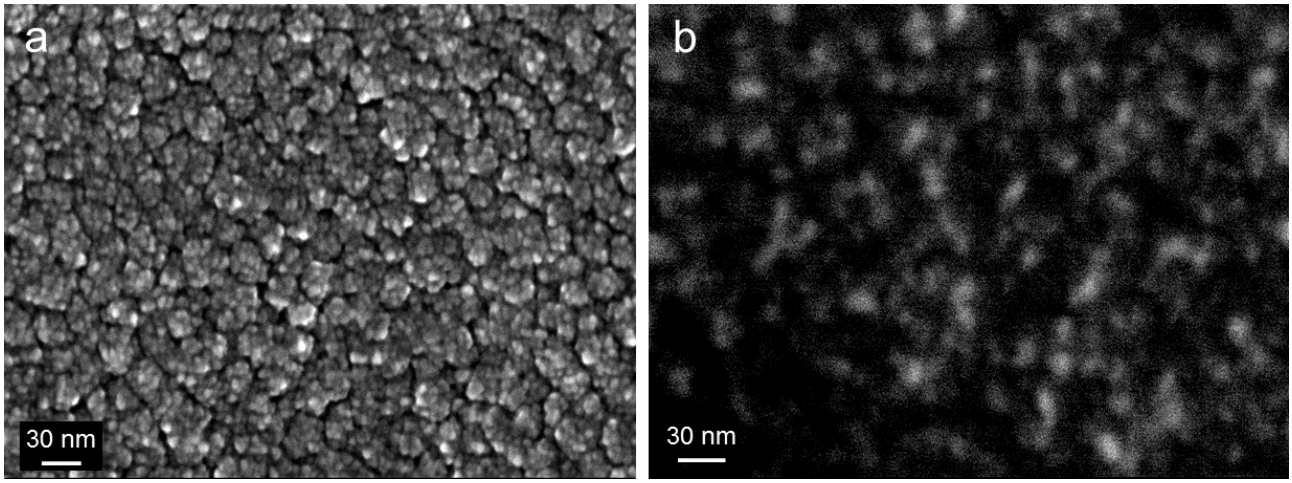
a
30 nm
b
30 nm

Fig. 4

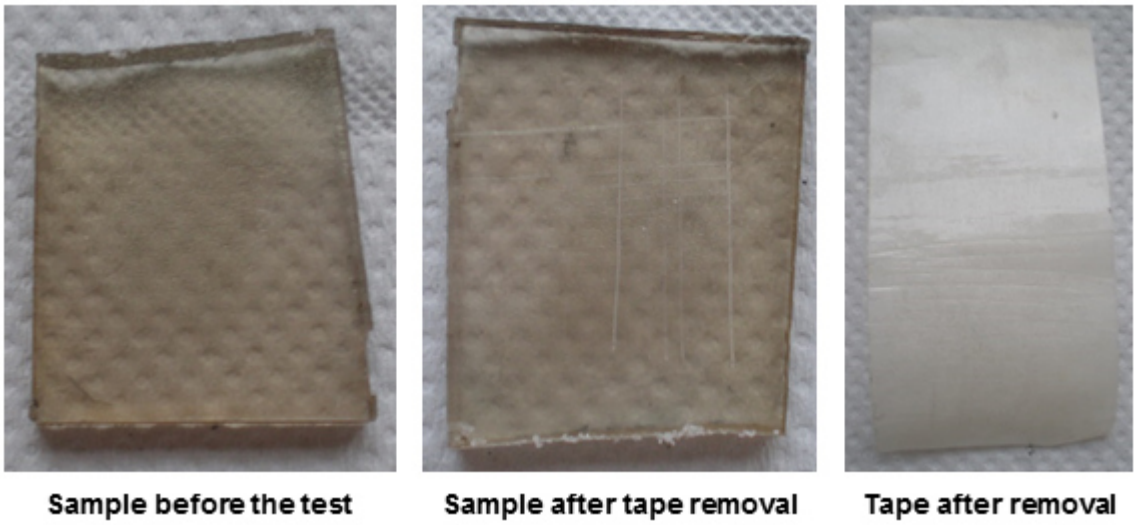
Sample before the test
Sample after tape removal
Tape after removal

Fig. 5

As deposited
Soaking for 48 h
Soaking for 14 days
Soaking for 28 days
15 min
40 mln

Fig. 6

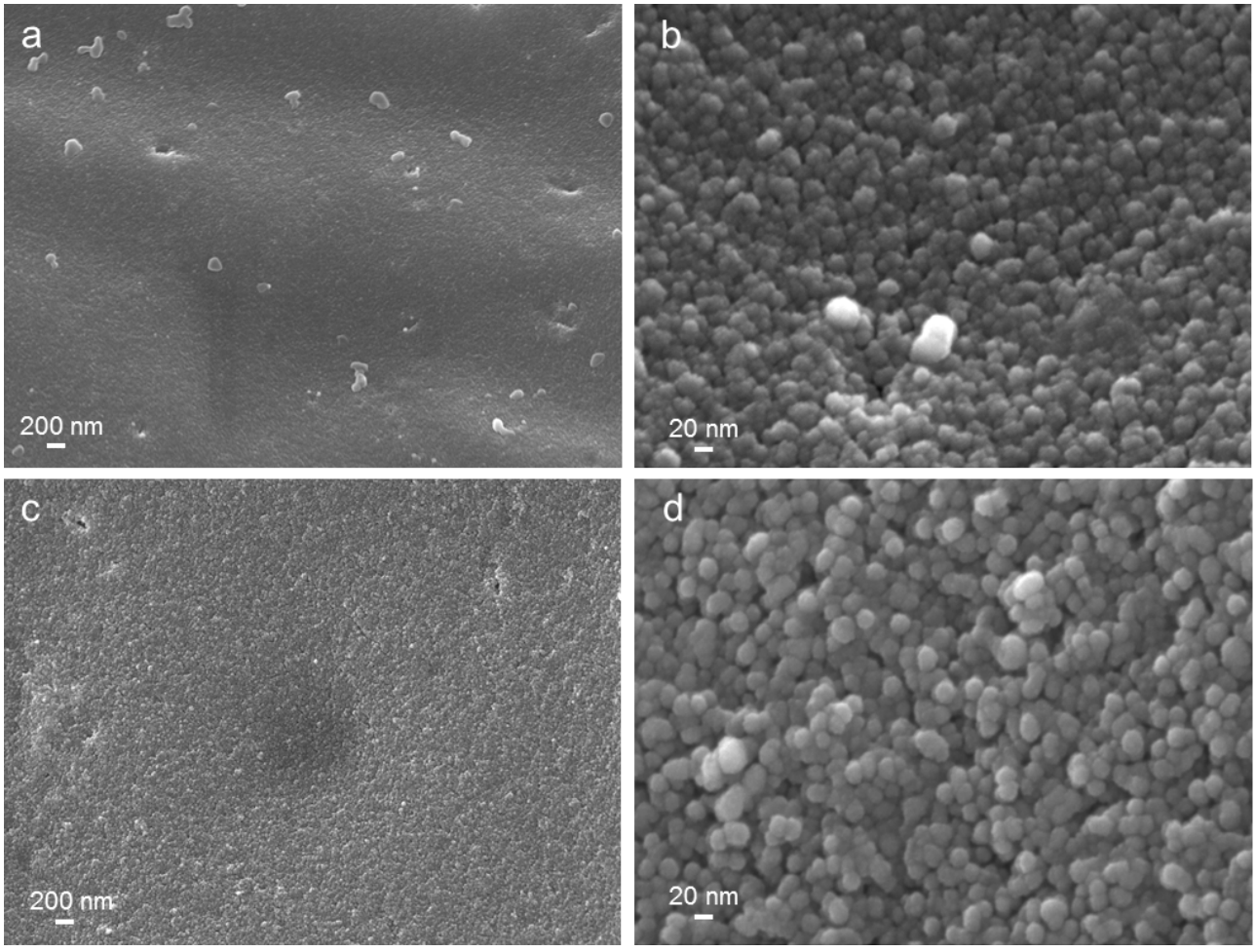
a
200 nm
b
20 nm
c
200 nm
d
20 nm

Fig. 7

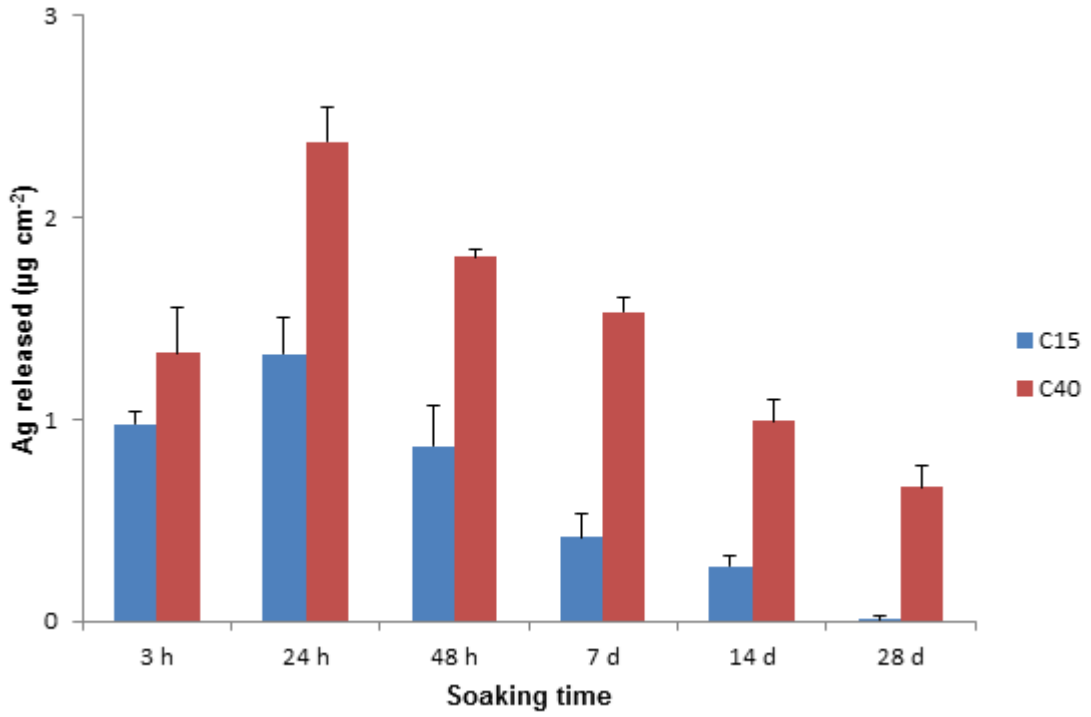
Ag released (µg cm-2)
3
2
1
0
3 h
24 h
48 h
7 d
14 d
28 d
Soaking time
C15
C40

Fig. 8

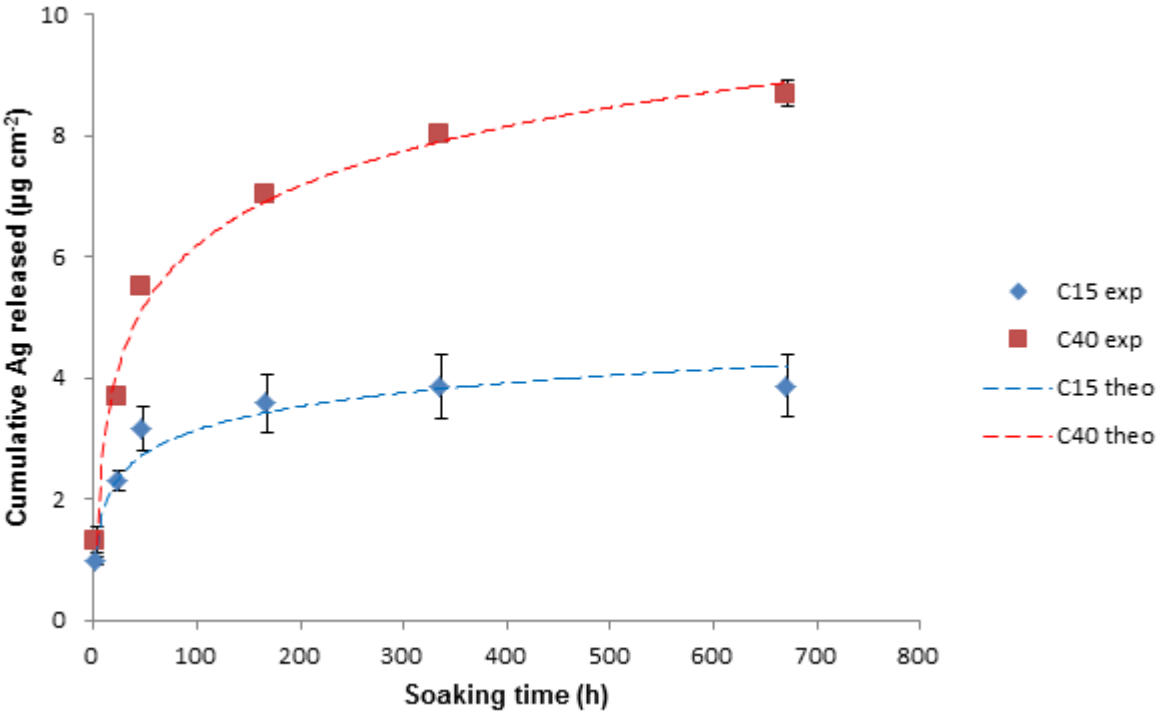
Cumulative Ag released (µg cm-2)
10
8
6
4
2
0
0
100
200
300
400
500
600
700
800
Soaking time (h)
C15 exp
C40 exp
C15 theo
C40 theo

Fig. 9

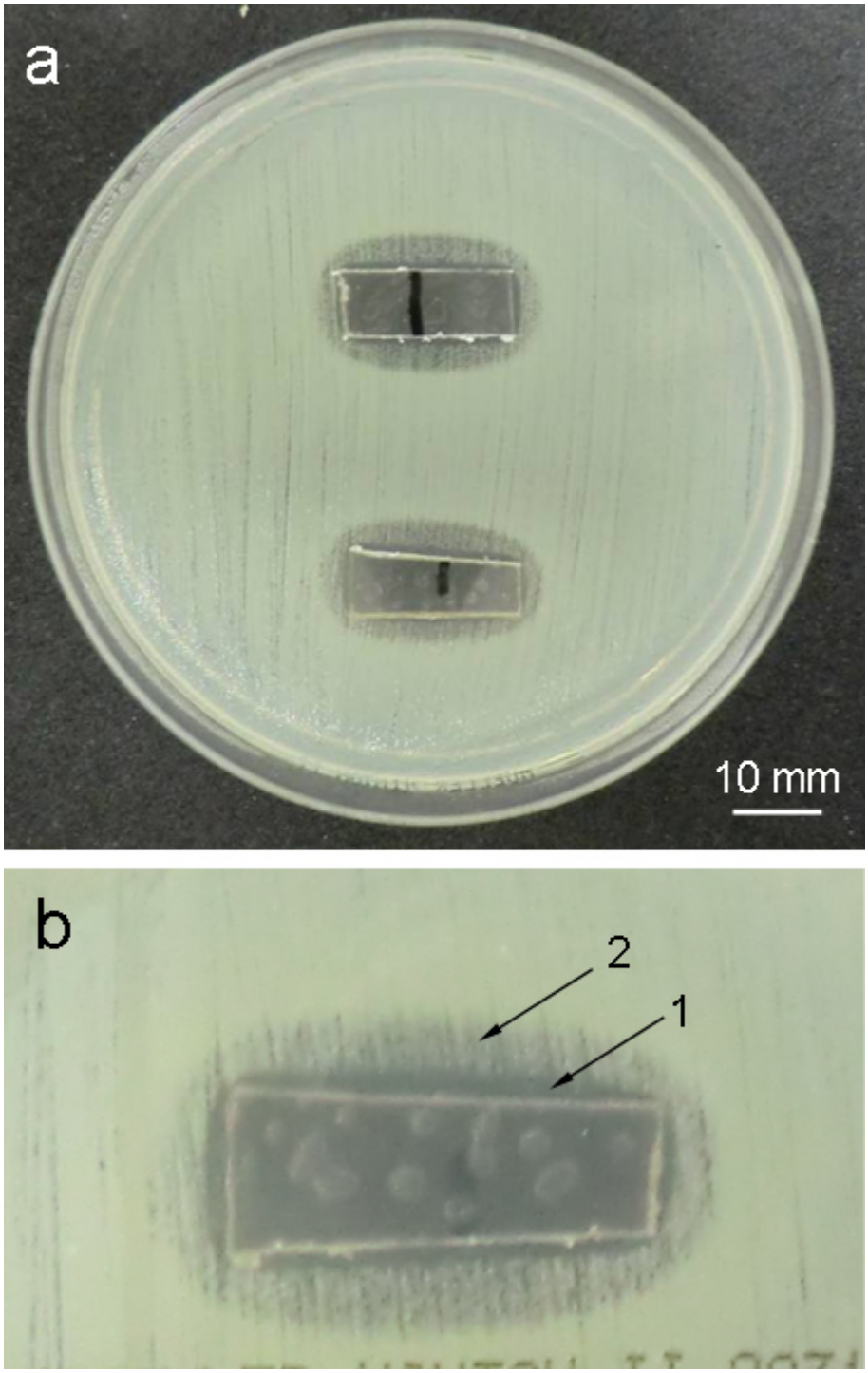

Fig. 10